Stacking fault related 3.31-eV luminescence at 130-meV acceptors in zinc oxide

M. Schirra,[1,*] R. Schneider,[1] A. Reiser,[1] G. M. Prinz,[1] M. Feneberg,[1] J. Biskupek,[2] U. Kaiser,[2] C. E. Krill,[3] K. Thonke,[1] and R. Sauer[1]

[1]*Institut für Halbleiterphysik, Universität Ulm, D-89069 Ulm, Germany*

[2]*Materialwissenschaftliche Elektronenmikroskopie, Universität Ulm, D-89069 Ulm, Germany*

[3]*Institut für Mikro- und Nanomaterialien, Universität Ulm, D-89069 Ulm, Germany*

(Received 19 July 2007; revised manuscript received 19 December 2007; published 26 March 2008)

Bulk ZnO samples, epitaxially grown ZnO layers, and ZnO nanostructures frequently exhibit a characteristic emission band at 3.31-eV photon energy whose origin is controversially discussed in the literature. Partly, this omnipresent band is ascribed to (e,A^0) transitions of conduction band electrons to acceptors, which are abundant in relatively high concentrations but have not positively been identified. The band is, in particular, often reported after intentional *p*-type doping of ZnO, preferentially with group V species. In the present work, we study the 3.31-eV band by low-temperature cathodoluminescence (CL) with high spatial resolution, by scanning electron microscopy, and by transmission electron microscopy (TEM). Line shape analyses at different temperatures give clear evidence that the band originates from an (e,A^0) transition where the acceptor binding energy is (130 ± 3) meV. The 3.31-eV luminescence is exclusively emitted from distinct lines on sample surfaces and cross sections representing intersections with basal planes of the wurtzite hexagons. Correlating monochromatic CL images with TEM images, we conclude that the localized acceptor states causing the 3.31-eV luminescence are located in basal plane stacking faults.

DOI: 10.1103/PhysRevB.77.125215 PACS number(s): 78.60.Hk, 78.55.Et, 68.37.Lp, 61.72.Nn

I. INTRODUCTION

The 3.31-eV emission band is a characteristic optical feature observed by photoluminescence and cathodoluminescence in a great variety of ZnO materials. It appears in nominally undoped bulk ZnO samples[1,2] as well as in ZnO nanostructures such as dots,[3] rods,[4,5] and powders.[6] It is also frequently observed in epitaxial layers grown by different growth methods, especially after intentional *p*-type doping with various dopant species, preferentially group V elements.[7–9]

This omnipresent luminescence band has been interpreted controversially, ascribing it, e.g., to donor-valence band transitions (D^0,h),[1] electron-hole recombination from donor-acceptor pairs (D^0,A^0),[4] electron-acceptor transitions (e,A^0),[5] recombination of excitons bound to deep neutral acceptors (A^0,X),[10] two-electron satellites of donor-bound excitons,[11,12] LO replicas of donor-bound excitons,[2] exciton recombination at silicon impurities,[13] or a "rotation domain structure-induced localized state bound exciton."[14]

In the majority of the pertinent works, it has been ascribed to transitions of free electrons to neutral acceptor states (e,A^0) with ionization energy close to 130 meV as deduced from the spectral position of the band.[15–19] This interpretation was in no case convincingly demonstrated as, e.g., by line shape analysis, and the structural or chemical origin of the acceptors remained unclarified so far. A straightforward association of the 3.31-eV band with substitutional acceptors introduced by intentional *p*-type doping might appear tempting but could be totally misleading.

In the present paper, we study the omnipresent 3.31-eV luminescence band in nominally undoped epitaxial ZnO films by low-temperature cathodoluminescence (CL) with high spatial resolution, by scanning electron microscopy (SEM), and by transmission electron microscopy (TEM). We first confirm, by detailed line shape analysis at different temperatures, that the band is a free-to-bound (e,A^0) transition appearing as a no-phonon transition (3.31 eV) and associated 1LO- and 2LO-phonon replicas. Other luminescence features in the spectra are also discussed. We then show that the 3.31-eV band is emitted exclusively from well-defined defect lines on the sample surface and on cross sections of the ZnO layer prepared for this investigation. High-resolution TEM of a cross section exhibits two types of defects: (i) basal plane stacking faults oriented perpendicular to the ⟨0001⟩ direction and (ii) defect lines parallel to the ⟨0001⟩ direction. In CL monochromatic images at 3.31-eV, the band is exclusively visible along directions perpendicular to ⟨0001⟩ and parallel to the stacking faults. We conclude that the acceptors under discussion reside in the basal plane stacking faults.

II. EXPERIMENT

The results reported here are obtained from three samples (1–3) selected out of many available samples, which were all grown in our group by a modified vapor phase epitaxy (VPE) process[20] on *a*-plane sapphire substrates. All samples have the same crystallographic orientation with respect to the *a*-plane sapphire substrate. Sample 1 consists of a smooth zinc oxide epitaxial layer approximately 3 μm thick, and was investigated by low-temperature CL in a modified SEM, by photoluminescence (PL), and by high-resolution x-ray diffraction (HRXRD). For characterization by CL, the sample was cleaved perpendicular to the *c* plane of the underlying *a*-plane sapphire substrate, resulting in smooth cleavage planes without requiring any postprocessing steps. Samples 2 and 3 have a layer thickness in the range of 0.5–1 μm, and the film surface is less smooth, showing a faceted structure. Sample 2 was only characterized by PL. Sample 3 was characterized by SEM-CL and prepared for TEM characterization by cutting the sample along the *c* plane of the underlying *a*-plane sapphire substrate. Thus, the cross section of sample 1 is perpendicular to the cross section of sample 3.

 ©2008 The American Physical Society

The CL setup is based on a scanning electron microscope (LEO DSM 982) with a heated field emitter cathode. The SEM is equipped with a He continuous-flow cryostat allowing sample temperatures in the range of 7–475 K. The CL signal is collected and coupled out by a glass fiber transparent in the near ultraviolet range. A home-made micropositioning mechanics allows us to locate the light-collecting tail of this fiber in a controlled way within a distance of a few tens of micrometer from the excitation spot of the incident electron beam. The glass fiber also allows flexible use of different detection systems: To record spectra with high resolution, the CL signal is dispersed by a monochromator with a focal length of 900 mm (Spex 1702/04) equipped with a 1200 rules/mm grating and detected by a LN_2-cooled charge coupled device (CCD) device with 1024×256 pixels of 25×25 μm^2 size. Alternatively, to record monochromatic CL images, a monochromator with a 250 mm focal length (Jobin Yvon HR 250) and a 1200 rules/mm grating in combination with a UV sensitive photomultiplier tube (PMT) (Hamamatsu R928) is used. The PMT output signal is amplified and fed into the auxiliary input of the SEM for image formation. The system allows recording of monochromatic CL images within the same time as necessary for recording a conventional SEM image in the slow-scan mode, i.e., typically in the range of seconds to a few hundreds of seconds. All monochromatic CL images were taken at a resolution of 512×512 pixels. The CL measurements were carried out at a rather low acceleration voltage of 2 kV, which allows a high lateral resolution below 50 nm limited by electron scattering in the crystal. The excitation current was 20–90 pA for the monochromatic CL images. Details of the setup with an estimate of the spatial resolution are described elsewhere.[21] Temperature-dependent CL measurements were also performed in the SEM at an acceleration voltage of 2 kV and a beam current of 700 pA. The signals were dispersed by the large monochromator (Spex 1702/04) and detected by a CCD camera.

Temperature-dependent PL measurements were carried out in a He continuous-flow cryostat by excitation with a HeCd laser (325 nm). The PL signal was dispersed by a monochromator (Spex 1704) with a 1 m focal length equipped with a 1200 rules/mm grating, and PL spectra were recorded with a LN_2-cooled CCD camera with 2000×800 pixels of 15×15 μm^2 size. The spectral resolution was better than 0.1 meV.

Thin cross sectional samples for the TEM investigations were prepared using standard techniques: Stripes of sandwiches were cut and glued together, then mechanically ground, dimpled, and polished down to thicknesses of less than 5 μm. Electron transparency of the sample was finally achieved by low angle ($<10°$) ion etching and ion polishing (0.5 to 5 kV) with a Fischione 1010 ion mill. Conventional TEM investigations (bright field, electron diffraction) were carried out on a Philips CM20 machine (200 kV operating voltage) equipped with a Gatan double tilt holder and a SiS KeenView slow-scan CCD camera. High-resolution TEM investigations were carried out on a FEI Titan 80-300 microscope (300 kV operating voltage) equipped with an aberration corrector for the objective lens (CEOS corrector), a Gatan double tilt holder, and a Gatan MC794 slow-scan CCD camera.

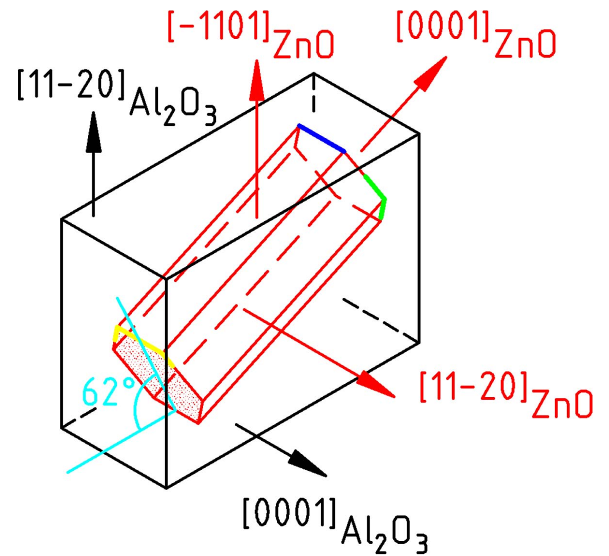

FIG. 1. (Color online) Crystal orientation of the ZnO epitaxial layer [having a $(\bar{1}101)$ surface] with respect to the *a*-plane sapphire substrate. The edges of the wurtzite hexagon in blue, green, and yellow represent the lines along which the 3.31-eV luminescence is observed.

HRXRD measurements were performed in a PANalytical X'Pert Pro diffractometer operated with Cu $K\alpha$ radiation ($\lambda = 1.54$ Å) in a Bragg-Brentano (Θ-2Θ) geometry.

III. RESULTS AND DISCUSSION

The following discussion is focused on sample 1 unless otherwise noted. Results obtained from sample 2 are discussed in context with the observation of a donor-acceptor pair transition (D^0,A^0). Sample 3 was preferentially investigated in transmission electron microscopy. In Sec. III A, we identify the electronic nature of the 3.31-eV band as a free-to-bound transition (e,A^0). This transition involves electrons from the conduction band recombining with holes localized at acceptor states. In Sec. III B, we focus on the acceptor states and show that they are induced by crystal defects associated with basal plane stacking faults. In Sec. IV, we discuss previously published data on the 3.31-eV emission, mainly in *p*-doped ZnO layers but also in nanostructures, in the light of the present findings suggesting that the omnipresent 3.31-eV luminescence is generally related to stacking faults.

To make the following discussion easier, we start by considering the crystal orientation of the investigated ZnO epitaxial layers with respect to the underlying *a*-plane sapphire substrate (Fig. 1). These findings were obtained by TEM and supported by HRXRD.

One *a* axis ($[11\bar{2}0]$ direction) of the zinc oxide film is oriented parallel to the $\langle 0001 \rangle$ direction of the *a*-plane sapphire substrate. The $[11\bar{2}0]$ direction of the sapphire substrate and the $\langle 0001 \rangle$ direction of the zinc oxide layer enclose an angle of $\approx 62°$. This orientation was confirmed by HRXRD measurements showing that the $(\bar{1}101)$ surface of

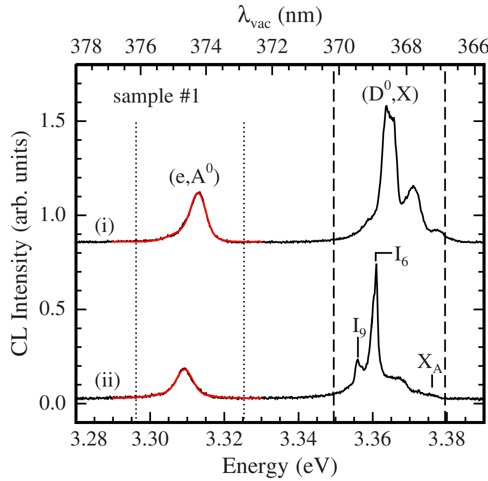

FIG. 2. (Color online) Integral CL spectra of sample 1 at $T=10$ K from (i) the surface and (ii) the cross section. The excited sample areas are shown in Figs. 7(a) and 7(d). The pairs of dashed and dotted lines delimit the spectral ranges used for the formation of the monochromatic CL images shown later in Figs. 7(b), 7(c), 7(e), and 7(f).

the zinc oxide film is oriented parallel to the $(11\bar{2}0)$ surface of the sapphire substrate. This crystallographic configuration is schematically shown in Fig. 1. The blue, green, and yellow edges of the wurtzite hexagon in Fig. 1 mark the lines along which the 3.31-eV band was observed with spatially resolved cathodoluminescence, as discussed in detail in Sec. III B.

For molecular beam epitaxy (MBE) grown layers, one typically finds the ZnO [0001] direction parallel to the a-plane sapphire $[11\bar{2}0]$ direction.[22] We obtain with our growth technique—depending on the growth parameters—ZnO layers either with the [0001] or the $[\bar{1}101]$ direction parallel to the a-plane $[11\bar{2}0]$ direction of the sapphire substrates.[20] The latter epitaxial relationship was discussed above and shown in Fig. 1.

A. Electronic nature of the 3.31-eV band

Figure 2 depicts CL spectra of sample 1 at 10 K integrated over areas of a few μm^2 taken from the surface (i) and from the cross section (ii). Both spectra show bound exciton (D^0,X) recombination near the band gap consisting of multiple lines and the luminescence band at 3.31-eV. The photon energies in the cross section spectrum (ii) are consistent with those quoted in the literature,[23] whereas the energies in the surface spectrum (i) are shifted by +3.7 meV. The shift indicates that compressive strain exists in the layer away from the cross section, which is relaxed close to it. This assumption appears natural as our cleavage produces defects [e.g., defect lines as seen in Fig. 7(d)–7(f)] promoting full relaxation. Experimentally, we can spatially resolve such differences since for the low acceleration voltage of 2 kV, the incoming electrons have a small penetration depth exciting only a thin (≤ 40 nm) layer.

The spectrum (ii) from the relaxed cross section exhibits prominently donor-bound exciton lines I_6 and I_9, which have been associated with the shallow donors Al and In, respectively.[23] In the present samples, both dopants are unintentionally introduced by trace contaminations of the source material. In the case of Al, an incorporation from the sapphire substrate is also likely.[21,24]

To identify the electronic nature of the transition at 3.31-eV, temperature-dependent CL measurements were carried out on the surface of sample 1 in a region of $10\times 10\ \mu m^2$ from 10 to 400 K. The data are shown for the range of 15–125 K in Fig. 3 (left panel). With increasing temperature, the high-energy Boltzmann tail of the transition at 3.31-eV becomes more pronounced. Furthermore, the associated LO-phonon replicas at 3.23 and 3.16 eV increase in relative intensity. These observations are typical for a free-to-bound transition, i.e., the recombination of an electron from the conduction band with a hole bound to an acceptor state, labeled (e,A^0).

The line shape of any free-to-bound transition such as (e,A^0) or (D^0,h) is basically given by the energy distribution of the free electrons (or holes) involved and can be described (without broadening) by

$$I(\hbar\omega,T) \sim \sqrt{\hbar\omega - [E_G(T) - E_A]}\exp\left(-\frac{\hbar\omega}{kT}\right). \quad (1)$$

Here, $I(\hbar\omega,T)$ is the measured intensity, $E_G(T)$ is the temperature-dependent band gap,[25] and E_A is the activation energy of the participating acceptor (or donor). Boltzmann statistics can be applied since in our case the quasi-Fermi level is close to the acceptor states. The ideal line shape of Eq. (1) must be convolved with the energy distribution of the involved acceptor states, which prevails at low temperatures as $I(\hbar\omega,T)$ in Eq. (1) has a full width at half maximum (FWHM) of $1.8kT$. The experimental line shape of the 3.31-eV band in Fig. 2 at 10 K is almost perfectly fitted by a superposition of two Gaussians. One Gaussian (of low intensity) is needed to reproduce the unsymmetric low-energy tail. The second, dominant Gaussian (FWHM $\approx$5 meV) reflects the acceptor energy distribution. At 25 and 55 K and at higher temperatures, the transition is well fitted by Eq. (1) convolved with this Gaussian (Fig. 4, $T=25$ K and $T=55$ K) whose FWHM remains nearly constant, amounting to $\approx$7 meV at 55 K. Therefore, the line shape is nearly symmetric up to 25 K where $1.8kT=3.9$ meV from Eq. (1). Finally, for temperatures above 90 K, lifetime broadening dominates, yielding good fits by Eq. (1) convolved with a Lorentzian (Fig. 4, $T=105$ K). For 25, 55, and 105 K, the fits yield an acceptor binding energy of $E_A=130\pm 3$ meV.

In the spectral region of the 3.31-eV transition, the first LO-phonon replicas of the free excitons X_A and X_B appear. Due to self-absorption, the replicas could be much stronger than the no-phonon free exciton recombination.[26] Therefore, we make sure by additional arguments that the 3.31-eV band is indeed an (e,A^0) transition as discussed and not the LO-phonon replica of X_A/X_B, which would also reveal relatively broad line shapes.

(i) The strongest argument for the above assignment is due to the spatial correlation of the (e,A^0) transition and its first LO-phonon replica at higher temperatures. We observed both transitions appearing at the same sample spots at 15 and

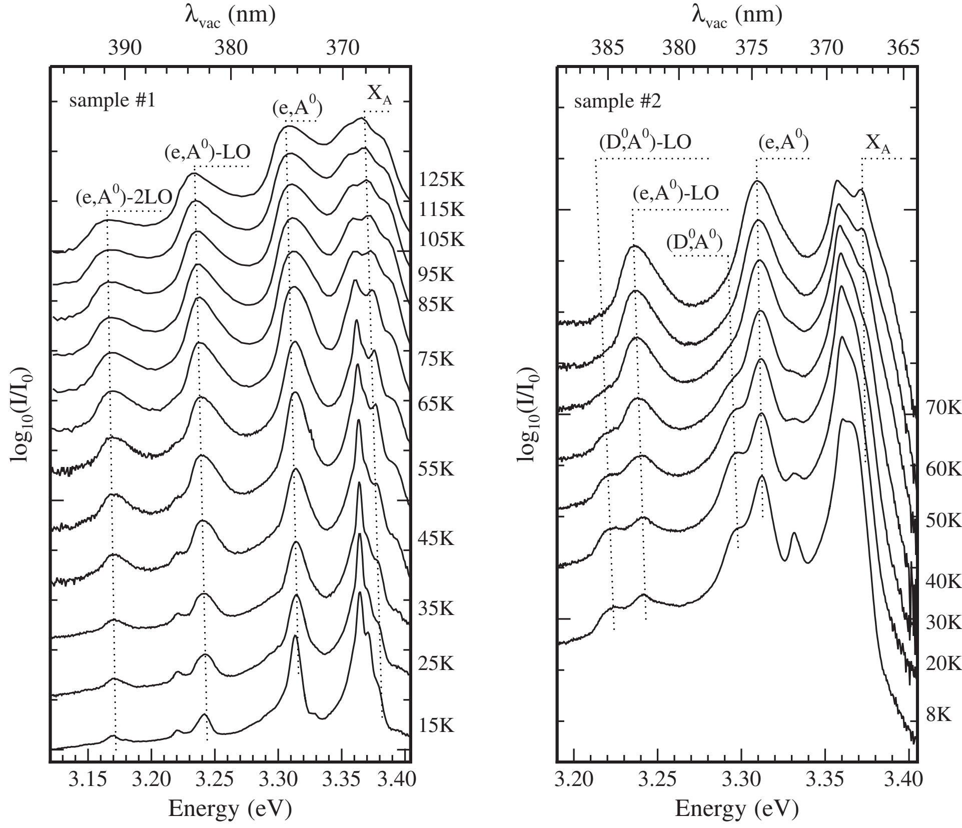

FIG. 3. Temperature dependence of the luminescence of sample 1 (left panel) and sample 2 (right panel).

75 K, respectively, as shown in Figs. 5(a)–5(c) by SEM-CL. Therefore, the (e,A^0) transition is a luminescence feature independent of the free exciton recombination. In contrast, in Figs. 5(d) and 5(e), the monochromatic CL images of the near-band-edge luminescence at 15 and 75 K, respectively, have identical dark dot patterns, which are completely different from the patterns of the (e,A^0) transitions.

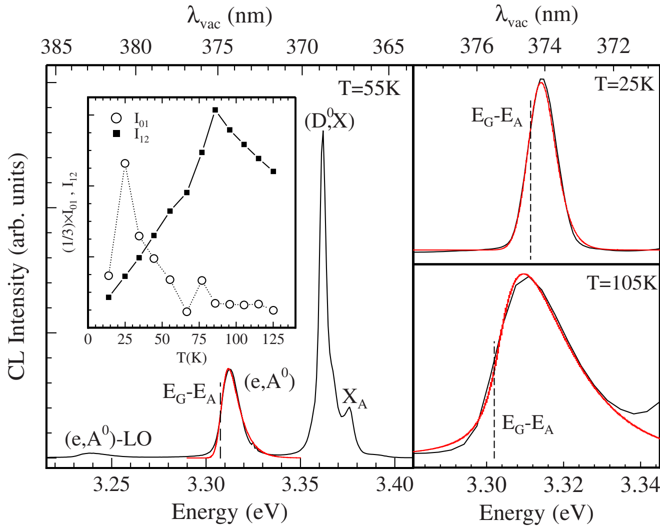

FIG. 4. (Color online) Left panel: selected spectrum (T=55 K) from Fig. 3 (left panel) and (in red) fit of the (e,A^0) transition by a convolution of a Gaussian with Eq. (1), as discussed in the text. The inset shows the temperature dependence of the ratios I_{01} and I_{12} also discussed in the text. Upper right panel: the (e,A^0) transition at 25 K and (in red) fit of the spectrum by a convolution of a Gaussian with Eq. (1). Lower right panel: the (e,A^0) line at 105 K and (in red) fit of the spectrum by a convolution of a Lorentzian with Eq. (1).

(ii) The LO-phonon replica of X_A should appear $\approx$5 meV below the 3.31-eV transition; hence, it could be well distinguished. The expected energy position of the LO-phonon replica of the X_B transition nearly matches the 3.31-eV line, but an intensity stronger than that of the LO replica of X_A is impossible. Therefore, the 3.31-eV line is an independent luminescence peak.

As an additional result, the inset in Fig. 4 shows the temperature dependence of the intensity ratio (labeled I_{01}) of the (e,A^0) transition to its 1LO-phonon replica and of the intensity ratio (labeled I_{12}) of the 1LO- to the 2LO-phonon replica,

$$I_{01} = \frac{\int I_{(e,A^0)}(\omega)d\omega}{\int I_{(e,A^0-LO)}(\omega)d\omega}, \quad (2)$$

$$I_{12} = \frac{\int I_{(e,A^0-LO)}(\omega)d\omega}{\int I_{(e,A^0-2LO)}(\omega)d\omega}. \quad (3)$$

We found that I_{12} is proportional to the temperature in the range of 15–85 K, whereas I_{01} behaves completely differently (see Fig. 4). In the same temperature range, the intensity ratio of the first to the second LO-phonon replica of the

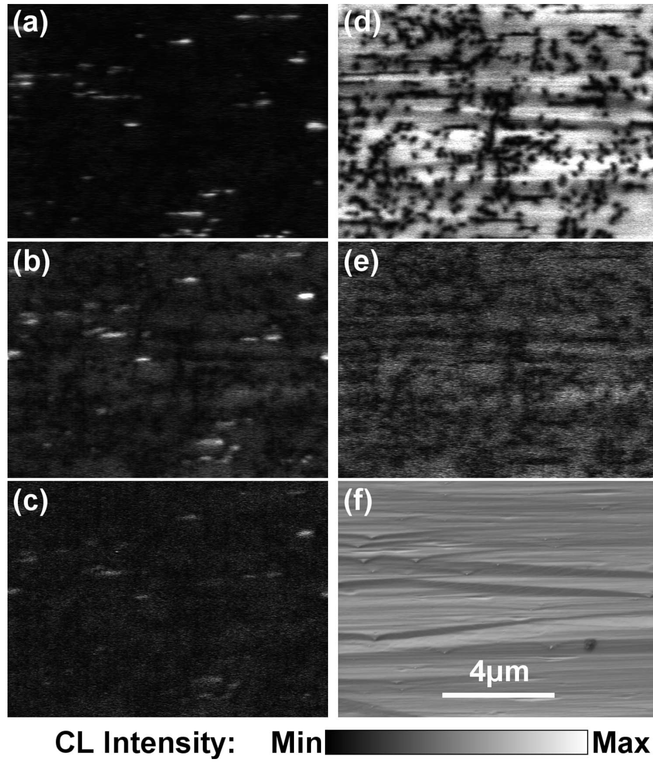

FIG. 5. (a) Monochromatic CL image recorded in the range of 3.296–3.325 eV (e,A^0) at 15 K, (b) at 75 K, and (c) monochromatic CL image of the $(e,A^0\text{-LO})$ transition at 75 K. (d) Monochromatic CL image of the near-band-edge luminescence (3.349–3.379 eV) recorded at 15 K, (e) at 75 K, and (f) corresponding SEM micrograph of the sample surface.

free exciton changes linearly with temperature.[26] Thus, the line at ≈3.24 eV cannot be the second LO replica of the free exciton lines, but must be the first LO replica of the 3.31-eV transition. Since I_{12} is found to be linearly dependent on the temperature, the coupling mechanism of LO phonons to the (e,A^0) recombination is apparently similar to the coupling of LO phonons to free excitons as described by Segall and Mahan.[27]

In our samples 1 and 3, we do not observe a (D^0,A^0) band, and even at low temperatures the (e,A^0) transition is dominant. Any concentration of donors is obviously overcompensated by acceptors. An estimate of the acceptor concentration N_A below yields high values of some 10^{18} cm^{-3}, consistent with the local appearance of the acceptors in conjunction with crystallographic defects (Sec. II).

A few samples—including sample 2—out of those which were grown do exhibit an extra transition 13 meV below the (e,A^0) band being likely a (D^0,A^0) band. The band is shown in Fig. 3 (right panel) at ≈3.30 eV. It disappears almost completely for temperatures above 50 K as the bound donor electrons in the transition initial state are thermally activated into the conduction band. A quantitative evaluation of the temperature dependence is shown in Fig. 6. A weak band at 3.22 eV photon energy in Fig. 3 (right panel) downshifted by the LO-phonon energy of ≈72 meV and following the pair band in its temperature dependence is ascribed to the LO-phonon replica of the pair band.

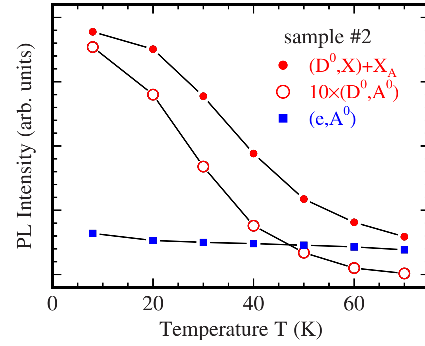

FIG. 6. (Color online) Temperature dependence of the (D^0,X), (D^0,A^0), and (e,A^0) transition intensities. The (D^0,A^0) and (e,A^0) lines were fitted by a Gaussian, and the intensity of the (D^0,X) transition was calculated by integrating the data from 3.34 to 3.39 eV. The error caused by the contribution of the free exciton X_A at higher temperatures is negligible.

The observation of free exciton luminescence at low temperatures in sample 1 (see Fig. 3, left panel) also supports our interpretation of the 3.30 eV line as a (D^0,A^0) transition since the intensity ratio of extrinsic, donor-bound exciton recombination to intrinsic, free exciton recombination is proportional to the corresponding impurity concentration.[29] In this case, it is indeed possible that the 1LO and 2LO replicas of the free excitonic recombination contribute to the spectrum in the range of the (e,A^0) band and its first LO replica. In the present case, this effect is negligible, as shown in Fig. 5 by the spatial dispersion of the discussed bands. In sample 2, no free exciton luminescence is found, suggesting that the donor concentration is higher than in sample 1. Thus, the probability of observing (D^0,A^0) transitions besides the (e,A^0) band is higher in sample 2 than in sample 1.

The spectral position of the (D^0,A^0) pair band serves to calculate the mean distance $\langle r_{AD}\rangle$ between the residual donors and the acceptors under discussion using the expression[28]

$$\hbar\omega_{DA} = E_G - E_A - E_D + \frac{e^2}{4\pi\epsilon_0\epsilon\langle r_{AD}\rangle}. \tag{4}$$

In Eq. (4), $\hbar\omega_{DA}$ is the peak energy of the donor-acceptor pair transition, E_G the fundamental band-gap energy, and E_A (E_D) the acceptor (donor) binding energy. The Coulomb energy term arises from the attraction between the ionized donor and acceptor cores. In zinc oxide, the fundamental band gap with respect to the A-valence band is 3.437 eV at low temperatures, and typical donors have binding energies in the range of 46–63 meV.[23] With an average donor binding energy of E_D=50 meV, an acceptor binding energy E_A =130 meV as derived above, and ϵ=8.6 for zinc oxide, we obtain an average donor-acceptor distance of $\langle r_{AD}\rangle \approx 4$ nm. Assuming a homogeneous distribution of donors and acceptors this leads to

$$N_{A/D} = \frac{3}{4\pi\langle r_{AD}\rangle^3} \tag{5}$$

for the higher concentration, N_A or N_D. Since the (e,A^0) transition is stronger in intensity than the (D^0,A^0) line, the

acceptor concentration exceeds the donor concentration, and therefore it is an acceptor concentration of $N_A \approx 4 \times 10^{18}$ cm^{-3}, which results from Eq. (5). As discussed in Sec. II, the acceptors turned out to be inhomogeneously distributed, appearing along crystallographic defects. Therefore, the above result for N_A should be considered only as a rough estimate for a three-dimensional equivalent concentration.

B. Structural origin of the (e,A^0) transition

Information on the local appearance and structural origin of the (e,A^0) transition was obtained, correlating monochromatic CL images with SEM and TEM images. In Fig. 7, the surface and a cross section of sample 1 are investigated. Compared in both cases are SEM [(a) and (d)] images with monochromatic CL images taken in the near-band-edge range of the X_A and (D^0,X) luminescence [(b) and (e)] and in the range of the (e,A^0) luminescence [(c) and (f)]. The corresponding sample orientation with respect to the crystallographic direction of the ZnO film and the *a*-plane sapphire substrate are as follows.

The bright lines [marked by blue boxes in Fig. 7(c)] correspond to the blue line in Fig. 1. The bright lines (marked by yellow boxes) in Fig. 7(f) belong to the yellow line in the cross section shown in Fig. 1. The kinks in the luminescence pattern include an angle of ≈60°. These kinks are observable due to the small angle of 28° between the basal plane of the ZnO epitaxial layer and the investigated cross section: Here, the penetration depth of the electron beam of ≈40 nm enables us to observe not only the straight-line projections on basal plane stacking faults but partly also luminescence from the kinked edges of the ZnO hexagon. These monochromatic CL images map the *c* plane of the wurtzite crystal structure of our ZnO layers.

The CL intensity patterns of the (e,A^0) band and the near-gap transitions in the range of 3.349–3.379 eV are complementary. This is particularly clearly seen in the images of Figs. 7(e) and 7(f). The (e,A^0) luminescence is confined to straight lines with kinks. Along these lines, near-band-edge luminescence is absent. In the surface images, the dark lines in Fig. 7(b) correspond to the direction of the grooves visible in the surface morphology in Fig. 7(a), and these lines are parallel to the cleaved edge of the sample. In Fig. 7(c), 3.31-eV light comes only from segments of straight lines, which are dark in Fig. 7(b), while near-gap luminescence is emitted from almost everywhere between these segments. Obviously, the electron-hole pairs generated by the electron beam can either recombine as free or donor-bound exciton transitions or are trapped along the lines to yield the (e,A^0) emission. Superimposed on the dark line structure in Fig. 7(b) is a stochastic pattern of dark spots, which is possibly due to dislocations, but has not been studied in detail in the present work.

The strictly localized appearance of the (e,A^0) transition suggests that it is correlated with the structural properties of our zinc oxide epitaxial layers. To further elucidate the nature of the bright lines, sample 3 was investigated by TEM. Prior to this investigation, it was made sure that this sample exhibits luminescence similar to sample 1. Also, complementary CL intensity patterns between the (e,A^0) band and the near-gap luminescence as in sample 1 were confirmed.

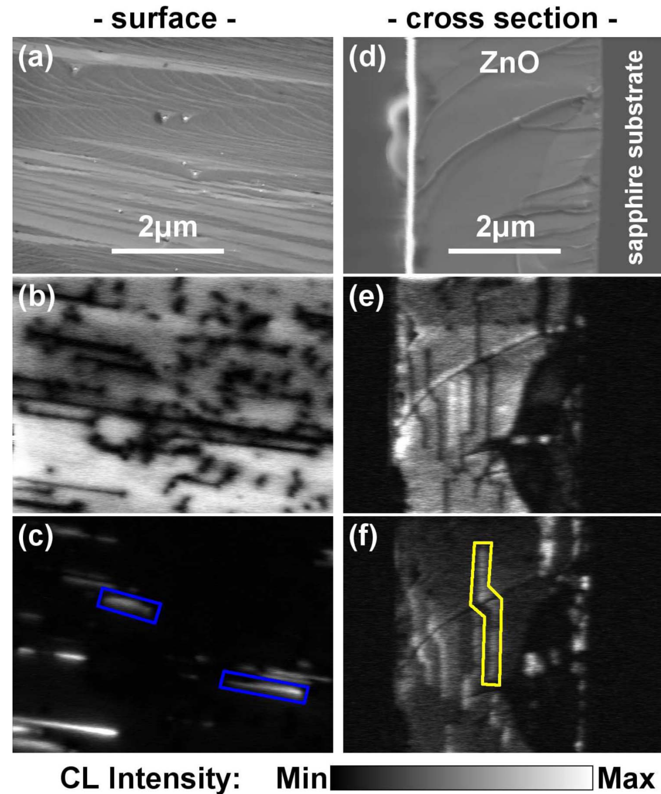

FIG. 7. (Color online) (a) SEM micrograph of the surface of sample 1. [(b) and (c)] Corresponding monochromatic CL images recorded in the ranges of 3.349–3.379 eV (near-gap transitions) and 3.296–3.325 eV [(e,A^0) transition], respectively. (d) SEM micrograph of the cross section of sample 1. [(e) and (f)] Corresponding monochromatic CL images in the same ranges as for (b) and (c), respectively. The blue and yellow frames in (c) and (f), respectively, indicate the corresponding crystal face marked in Fig. 1.

The morphology of a sample cross section was studied by TEM. Figure 8(a) exhibits in bright field imaging a network of intersecting defect lines parallel or perpendicular to the *c* axis (⟨0001⟩ direction) of the ZnO film. A high-resolution TEM image of the cross section [Fig. 8(b)] shows again these two types of defects. In Fig. 8(c), we observed the (e,A^0) band along the box marked in green, which corresponds to the green line in the schematics of Fig. 1. The lines perpendicular to the *c* axis of the ZnO layer are basal plane stacking faults intersecting the sample cross section. They have been studied in more detail with aberration-corrected high-resolution TEM, as shown in Fig. 9(a). The defects are positively identified as stacking faults by Fourier filtering of the ZnO {0001} lattice planes performed to enhance the contrast and to obtain an improved image of the defects along the basal plane [see Fig. 9(b)]. The filtered image clearly shows interjected half-planes in the lattice as marked by arrows representing stacking faults. The microscopic origin of the defect lines parallel to the *c* axis of the ZnO film is presently not clear and has not been studied here.

Comparing TEM and SEM-CL, the structural data can be correlated with luminescence data. Luminescence in the

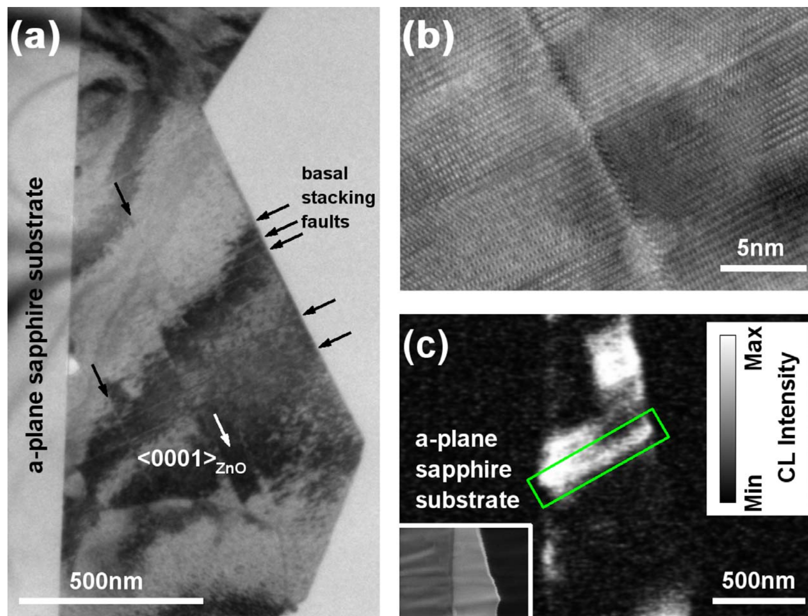

FIG. 8. (Color online) (a) TEM bright-field image of sample 3, (b) high-resolution TEM image of the observed dislocations, and (c) monochromatic CL image of the (e,A^0) transition in the range of 3.295–3.332 eV also recorded from sample 3. The inset in (c) shows the corresponding SEM micrograph. All ZnO crystal orientations in (a)–(c) are identical.

spectral range of the (e,A^0) transition is exclusively observed along lines perpendicular to the ZnO c axis or, respectively, parallel to the lines associated with the stacking faults. Hence, the acceptor states are confined to these defects. As Figs. 7(c), 7(f), and 8(c) had shown, the luminescence patterns are oriented parallel to the whole set of all equivalent $\langle 11\bar{2}0\rangle$ directions of the ZnO epitaxial layer, which lies in the basal plane of the crystal hexagon. It is therefore clear *that the acceptors under discussion are located in the basal plane stacking faults*.

Stacking faults have been shown in other materials to give rise to luminescence, as e.g., in GaN,[30,31] whereas dislocations act as nonradiative defects in III-V compounds[32,33] and in II-VI compounds.[34] Therefore, we tentatively ascribe the dark spot pattern in Fig. 7(b) to dislocation lines penetrating the surface.

IV. POSSIBLE IMPLICATIONS OF THE RESULTS

The luminescence band under investigation has often been reported in all kinds of ZnO samples reaching from bulk material over epitaxial layers to nanorods and nanodots. Since it is related to a high local density of acceptor states, which we have associated above with stacking faults, such defects might play a vital role for the electrical properties of all kinds of ZnO materials. In the following existing literature data on the 3.31-eV band are reviewed and critically discussed.

A band located at 3.304 eV at $T=100$ K was reported in studies on Eagle Picher substrate material by Wang and Giles[35] and Hamby *et al.*[36] It became dominant in the PL spectra at higher temperatures and was interpreted as LO-assisted free exciton X_A recombination, although the authors recognized that the energy spacing from the no-phonon transmission was by some meV too small and that at higher temperatures the intensity was orders of magnitudes higher than that of the X_A transition itself. Both groups also observed that the redshift of this band with temperature was less than that of the X_A lines. They found the shift to be $3kT/2$. Using the low-temperature band-gap energy, the data can indeed be fitted much better with a shift of $kT/2$, hinting to a free-to-bound transition.

One of the first reports of PL data from intentionally p-doped ZnO was published by Look *et al.*[19] After doping with nitrogen, the homoepitaxial ZnO layers grown by mo-

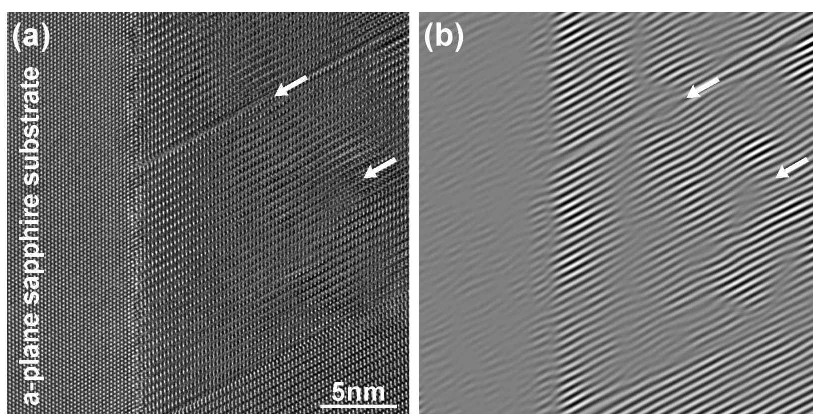

FIG. 9. (a) Aberration-corrected high-resolution TEM image of sample 3 showing the interface of the substrate and the ZnO epitaxial layer. (b) Fourier-filtered image of (a) using the ZnO {0001} lattice planes with enhanced defect contrast; especially interjected planes can be clearly seen and are marked by arrows in (a) and (b). The sample orientation in (a) and (b) is identical to that of Fig. 8.

lecular beam epitaxy showed a band at 3.315 eV as the dominant feature. The band was by a factor of ≈1300 lower in intensity than the near-gap excitonic processes seen as the dominant emission in an undoped reference sample. This showed that nonradiative recombination caused by defects was important and quenched the excitonic processes. Although in this work[19] the band was interpreted as an acceptor-bound exciton (A^0,X) recombination, it might alternatively consist of stacking fault related (e,A^0) emission as investigated in the present work. The acceptor concentration quoted to be only $\approx 10^{17}$ cm^{-3} and obtained from Van der Pauw–Hall measurements was unexpectedly low. If stacking faults were involved, they would cause local band bending and inhomogeneous hole accumulation, and Hall data would become highly unreliable, fluctuating between *n* type and *p* type in the same layer. Such alternating behavior has indeed frequently been observed in nominally *p*-type doped samples[10,37–40]

Hwang *et al.*[15] used rf magnetron sputtering for the production of phosphorus-doped ZnO films. The most prominent feature in their spectra was a band at 3.31 eV, which was ascribed to a free-electron-to-acceptor transition. For the acceptor, a binding energy of 127 meV was derived. Again, it appears questionable whether the (e,A^0) transition observed from these samples was due to the phosphorus dopants, which were intentionally introduced, or whether stacking faults due to nonideal growth conditions can be made responsible for this luminescence.

Similarly, Ye *et al.*[16] introduced phosphorus in their ZnO metal organic VPE (MOVPE) growth process either by adding PH_3 or by codoping with phosphorus and indium. At least for the codoped sample, a strong PL signal at 3.315 eV was found, which was ascribed to an (e,A^0) transition by the authors. For the acceptor involved, a binding energy of 123 meV was derived. One might wonder whether the dopant phosphorus, amounting to a 1.5% concentration in the samples, was exclusively responsible for the *p*-type conductivity reported. The same authors also reported changes in the Raman spectrum of phosphorus-doped ZnO.[41] The changes were ascribed to “disorder-activated modes” and the “variation of short-range forces in ZnO uniaxial lattice caused by phosphorus incorporation.” It appears feasible that the observed changes were induced by a relatively high density of stacking faults.

Xiu *et al.*[10] found varying *n*- and *p*-type conductivities in their MBE grown ZnO doped with phosphorus from a GaP effusion cell, which depended on the oxygen concentration and the temperature of the effusion cell. For a sample with *p*-type Hall conductivity, the PL spectrum exhibited a dominant band at 3.315 eV, which the authors interpreted as originating from a bound exciton (A^0,X). It was peculiar that increased temperatures of the GaP effusion cell, expected to increase the phosphorus concentration, did not lead to clear *p*-type conductivity in Hall measurements and resulted in a lower PL intensity of the 3.315 eV band. It is tempting to suspect that, also in this case, the formation of stacking faults related to the appearance of the 3.315 eV band played an unrecognized role. The same group of authors later reported PL spectra of ZnO:P layers, where again a broad peak at 3.319 eV was found to dominate the spectrum.[42]

As an alternative *p*-type dopant to P, Xiu *et al.*[17] doped their MBE grown ZnO epitaxial layers with Sb. After annealing, they found a saturation of the electrically active acceptor concentration at around 1.8×10^{18} cm^{-3}. Their PL spectra exhibited DAP and (e,A^0) bands, and an activation energy of $E_A=140$ meV for the acceptors was obtained. Within the error margin their value is the same as that found for the stacking fault related acceptor states.

Ryu *et al.*[43,44] observed in their As-doped ZnO layers grown by pulsed laser deposition (PLD) on GaAs substrates a PL band at ≈3.32 eV increasing in strength with the As concentration, which they interpreted as acceptor-bound exciton luminescence. Similarly, Look *et al.*[45] found a broad PL band at 3.31 eV, which they also assigned to (A^0,X) transitions. Kang *et al.*[18] observed in ZnO on GaAs substrates a change from *n*-type to *p*-type conductivity after annealing at 500 °C, and ascribed it to the diffusion of arsenic from the GaAs substrate into the ZnO layer. In the PL spectrum of the annealed layer, a band at 3.34 eV was associated with an (A^0,X) transition, and a band at ≈3.30 eV with (e,A^0) emission. Anew one might wonder whether stacking faults could develop during the annealing process, introducing related acceptor states.

In this context, scanning capacitance measurements carried out by von Wenckstern *et al.*[46] on homoepitaxial PLD-grown phosphorus-doped ZnO layers reveal a remarkable detail: In regions with defects, the authors find *p*-type conductivity, whereas regions without defects are *n* type. This peculiar observation might find an explanation in terms of stacking fault-related acceptors.

The 3.31-eV PL band has not only been observed in conjunction with intentional *p*-type doping. Fujita and Nakai[47] found the band at large intensities in ZnO samples grown by MOVPE when di-isopropylzinc or tertiary butanol with high VI/II ratio was used as a Zn source. Also, the band appeared in ZnO nanostructures such as small-sized ZnO quantum dots about 4 nm in diameter (Fig. 5 in Fonoberov *et al.*[3]). Most likely, the 3.31-eV band is again an (e,A^0) transition—albeit interpreted as an (A^0,X) emission by the authors—since the band shows an upshift of $kT/2$ relative to the band gap, consistent with the change in kinetic energy of free electrons in an (e,A^0) transition. In the work of Fonoberov *et al.*[3] the 3.31-eV band was ascribed to surface-related acceptor states. We rather feel that stacking faults might again be the origin of the luminescence.

Similarly, in a recent PL study of different ZnO powders with particle sizes between 70 and 380 nm, a band at ≈3.31 eV showed up, which was ascribed to surface excitons.[6] This band dominated the PL spectra at room temperature. The temperature dependence of the emission energy was identical to that which we observe for the present 3.31-eV (e,A^0) transition. These features speak for an (e,A^0) interpretation of the band and might hint at stacking faults in the ZnO powders.

In contrast to all these cases, ZnO nanopillars grown on sapphire substrates by the vapor-liquid-solid process at high temperatures do not show PL emission at 3.31 eV in regions of regular hexagonal growth and are absolutely defect free in TEM studies.[48] However, nanopillars grown on silicon seem to be less perfect and do show this band.[49] A further example

are ZnO rods grown by MOVPE at relatively low temperature (≈500 °C) on sapphire:[4] A pronounced PL band at 3.315 eV emerged and was interpreted as DAP luminescence. In the light of our discussion, it appears reasonable to assume that in these rods having ill-defined shapes, stacking faults are present in high concentrations.

The introduction of group V dopants could lower the threshold for stacking fault formation—e.g., by the generation of local strain—or could kinetically favor their appearance. Theoretical calculation predict a rather low formation enthalpy of only 15–47 meV/unit cell area for stacking faults in ZnO.[50] Therefore, group V dopants could produce stacking faults that according to our results, act as acceptors, but lead to very low mobilities and strong spatial fluctuations of the doping levels. Hence, the observation of the 3.31-eV band does not necessarily imply that successful p doping by substitutional acceptors has been achieved. Also, Hall measurements can yield spurious results and are only reliable if a low density of stacking faults is verified by other experimental methods.

V. CONCLUSION

In summary, the electronic nature and the structural origin of the omnipresent 3.31-eV luminescence band in zinc oxide epitaxial films have been studied. The electronic nature is unambiguously identified as a free-to-bound (e,A^0) transition of electrons from the conduction band to holes localized at relatively shallow acceptor states. The hole binding energy of the acceptors is (130 ± 3) meV, and their local concentration amounts to $\approx 4\times10^{18}$ cm^{-3}, overcompensating uncontrolled donor concentrations of typically some 10^{17} cm^{-3} and suppressing neutral-donor-bound exciton (D^0,X) recombination and (D^0,A^0) recombination in the vicinity of the acceptors.

The (e,A^0) transition is found to appear exclusively along distinct lines visible on the sample surface and on two cross sections that are perpendicular to each other. Combining these results from spatially resolved CL with TEM images, we conclude that the bright lines are intersections of basal plane stacking faults with the surface and the cross sections and that the acceptorlike defects are located in the basal plane stacking faults. Stacking faults have been predicted theoretically to form rather easily due to their low formation energy.[50] The microscopic structure of the acceptor states remains unknown. An agglomeration of doping impurities or other species at the defects seems less probable since the high acceptor concentration would require too high an amount of such species. Dangling bonds which can form localized electronic states would then be more probable candidates for the acceptorlike defect states.

Our results imply that the correct interpretation of the luminescence band at around 3.31 eV in terms of an (e,A^0) transition is not necessarily an indication for a successful p-type doping of ZnO.

ACKNOWLEDGMENTS

The present work was financially supported by the Kompetenznetzwerk “Funktionelle Nanostrukturen” within the “Landesstiftung” program of the Federal Government of the State of Baden-Württemberg.

*martin.schirra@uni-ulm.de

[1] M. R. Wagner, P. Zimmer, A. Hoffmann, and C. Thomsen, Phys. Status Solidi (RRL) **1**, 169 (2007).
[2] X. Wang, H. Iwaki, M. Murakami, X. Du, Y. Ishitani, and A. Yoshikawa, Jpn. J. Appl. Phys., Part 2 **42**, L99 (2003).
[3] V. A. Fonoberov, K. A. Alim, A. A. Balandin, F. Xiu, and J. Liu, Phys. Rev. B **73**, 165317 (2006).
[4] B. P. Zhang, N. T. Binh, Y. Segawa, K. Wakatsuki, and N. Usami, Appl. Phys. Lett. **83**, 1635 (2003).
[5] Q. X. Zhao, M. Willander, R. E. Morjan, Q.-H. Hu, and E. E. B. Campbell, Appl. Phys. Lett. **83**, 165 (2003).
[6] J. Fallert, R. Hauschild, F. Stelzl, A. Urban, M. Wissinger, H. Zhou, C. Klingshirn, and H. Kalt, J. Appl. Phys. **101**, 073506 (2007).
[7] D. C. Look and B. Claflin, Phys. Status Solidi B **241**, 624 (2004).
[8] D. C. Look, Semicond. Sci. Technol. **20**, S55 (2005).
[9] D. C. Look, Mater. Res. Soc. Symp. Proc. **957**, K08–05 (2007).
[10] F. X. Xiu, Z. Yang, L. J. Mandalapu, and J. L. Liu, Appl. Phys. Lett. **88**, 152116 (2007).
[11] J.-R. Duclère, B. Doggett, M. O. Henry, E. McGlynn, R. T. Rajendra Kumar, J.-P. Mosnier, A. Perrin, and M. Guilloux-Viry, J. Appl. Phys. **101**, 013509 (2007).
[12] C. Liu, S. H. Chang, T. W. Noh, J.-H. Song, and J. Xie, Phys. Status Solidi B **244**, 1528 (2007).
[13] M. Fujita, N. Kawamoto, T. Tatsumi, K. Yamagishi, and Y. Horikoshi, Jpn. J. Appl. Phys., Part 1 **42**, 67 (2003).
[14] K. Iwata, P. Fons, S. Niki, A. Yamada, K. Matsubara, K. Nakahara, T. Tanabe, and H. Takasu, J. Cryst. Growth **214-215**, 50 (2000).
[15] D.-K. Hwang, H.-S. Kim, J.-H. Lim, J.-Y. Oh, J.-H. Yang, S.-J. Park, K.-K. Kim, D. C. Look, and Y. S. Park, Appl. Phys. Lett. **86**, 151917 (2005).
[16] J. D. Ye, S. L. Gu, F. Li, M. Zhu, R. Zhang, Y. Shi, Y. D. Zheng, X. W. Sun, G. Q. Lo, and D. L. Kwong, Appl. Phys. Lett. **90**, 152108 (2007).
[17] F. X. Xiu, Z. Yang, L. J. Mandalapu, D. T. Zhao, and J. L. Liu, Appl. Phys. Lett. **87**, 252102 (2005).
[18] H. S. Kang, G. H. Kim, D. L. Kim, H. W. Chang, B. D. Ahn, and S. Y. Lee, Appl. Phys. Lett. **89**, 181103 (2006).
[19] D. C. Look, D. C. Reynolds, C. W. Litton, R. L. Jones, D. B. Eason, and G. Cantwell, Appl. Phys. Lett. **81**, 1830 (2002).
[20] A. Reiser *et al.* (unpublished).
[21] M. Schirra, A. Reiser, G. M. Prinz, A. Ladenburger, K. Thonke, and R. Sauer, J. Appl. Phys. **101**, 113509 (2007); Virtual J. Nanoscale Sci. Technol. **15**, No. 24 (2007).
[22] P. Fons, K. Iwata, A. Yamada, K. Matsubara, S. Niki, K. Nakahara, T. Tanabe, and H. Takasu, Appl. Phys. Lett. **77**, 1801

(2000).
[23] B. K. Meyer, H. Alves, D. M. Hofmann, W. Kriegeis, D. Forster, F. Bertram, J. Christen, A. Hoffmann, M. Strassburg, M. Dworzak, U. Haboeck, and A. V. Rodina, Phys. Status Solidi B **241**, 231 (2004).
[24] T. Nobis, E. M. Kaidashev, A. Rahm, M. Lorenz, J. Lenzer, and M. Grundmann, Nano Lett. **4**, 797 (2004).
[25] A. Schildknecht and K. Thonke (private communication).
[26] C. Klingshirn, Phys. Status Solidi B **71**, 547 (1975).
[27] B. Segall and G. D. Mahan, Phys. Rev. **171**, 935 (1968).
[28] D. G. Thomas, M. Gershenzon, and F. A. Trumbore, Phys. Rev. **133**, A269 (1964).
[29] M. Tajima, Appl. Phys. Lett. **32**, 719 (1978).
[30] J. Mei, S. Srinivasan, R. Liu, F. A. Ponce, Y. Narukawa, and T. Mukai, Appl. Phys. Lett. **88**, 141912 (2006).
[31] T. Gühne, Z. Bougriouna, P. Vennéguès, M. Leroux, and M. Albrecht, J. Appl. Phys. **101**, 113101 (2007).
[32] H. Kanie, K. Sugimoto, and H. Okada, Phys. Status Solidi A **188**, 481 (2001).
[33] N. Pauc, M. R. Philips, V. Aimez, and D. Droubin, Appl. Phys. Lett. **89**, 161905 (2006).
[34] J.-M. Bonard, J.-D. Ganière, L. Vanzetti, J. J. Paggel, L. Sorba, A. Franciosi, D. Hervé, and E. Molva, J. Appl. Phys. **83**, 1945 (1998).
[35] L. Wang and N. C. Giles, J. Appl. Phys. **94**, 973 (2003).
[36] D. W. Hamby, D. A. Lucca, M. J. Klopfstein, and G. Cantwell, J. Appl. Phys. **93**, 3214 (2003).
[37] M. Joseph, H. Tabata, H. Saeki, K. Ueda, and T. Kawai, Physica B **302**, 140 (2001).
[38] Xin-Li Guo, H. Tabata, and T. Kawai, Opt. Mater. (Amsterdam, Neth.) **19**, 229 (2002).
[39] X. Li, Y. Yan, T. A. Gessert, C. L. Perkins, D. Young, C. DeHart, M. Young, and T. J. Coutts, J. Vac. Sci. Technol. A **21**, 1342 (2003).
[40] D. C. Look (private communication); M. A. Reshchikov (private communication).
[41] J. D. Ye, S. L. Gu, S. M. Zhu, S. M. Liu, Y. D. Zheng, R. Zhang, Y. Shi, Q. Chen, H. Q. Yu, and Y. D. Ye, Appl. Phys. Lett. **88**, 101905 (2006).
[42] F. X. Xiu, Z. Yang, L. J. Mandalapu, and J. L. Liu, Mater. Res. Soc. Symp. Proc. **892**, FF18–09 (2006).
[43] Y. R. Ryu, S. Zhu, D. C. Look, J. M. Wrobel, H. M. Jeong, and H. W. White, J. Cryst. Growth **216**, 330 (2000).
[44] Y. R. Ryu, T. S. Lee, and H. W. White, Appl. Phys. Lett. **83**, 87 (2003).
[45] D. C. Look, G. M. Renlund, R. H. Burgener II, and J. R. Sizelove, Appl. Phys. Lett. **85**, 5269 (2004).
[46] H. von Wenckstern, G. Benndorf, S. Heitsch, J. Sann, M. Brandt, H. Schmidt, J. Lenzner, M. Lorenz, A. Y. Kuznetsov, B. K. Meyer, and M. Grundmann, Appl. Phys. A: Mater. Sci. Process. **88**, 125 (2007).
[47] Y. Fujita and R. Nakai, J. Cryst. Growth **272**, 795 (2004).
[48] A. Reiser, A. Ladenburger, G. M. Prinz, M. Schirra, M. Feneberg, A. Langlois, R. Enchelmaier, Y. Li, R. Sauer, and K. Thonke, J. Appl. Phys. **101**, 054319 (2007).
[49] Y. Li, M. Feneberg, A. Reiser, M. Schirra, R. Enchelmaier, A. Ladenburger, A. Langlois, R. Sauer, and K. Thonke, J. Appl. Phys. **99**, 054307 (2006); Virtual J. Nanoscale Sci. Technol. **13**, No. 11 (2006).
[50] Y. Yan, G. M. Dalpian, M. M. Al-Jassim, and S.-H. Wei, Phys. Rev. B **70**, 193206 (2004).